Chinese Journal of Oceanology and Limnology
Vol. 26 No. 4, P. 440-449, 2008
DOI: 10.1007/s00343-008-0440-6

The atmospheric wet pool: definition and comparison with the oceanic warm pool*

ZHANG Caiyun (张彩云) [†,††,**], CHEN Ge (陈戈) [††]
[†] *Program of Geospatial Information Sciences, University of Texas at Dallas, TX 75083, USA*
[††] *Ocean Remote Sensing Institute, Ocean University of China, Qingdao 266100, China*

Received January 19, 2007; revision accepted July 15, 2008

Abstract The oceanic warm pool (OWP) defined by sea surface temperature (SST) is known as the "heat reservoir" in the ocean. The warmest portion in the ocean mirrors the fact that the wettest region with the largest accumulation of water vapor (WV) in the atmosphere, termed atmospheric wet pool (AWP), should be identified because of the well-known Clausius-Clapeyron relationship between SST and WV. In this study, we used 14-year simultaneous observations of WV and SST from January 1988 to December 2001 to define the AWP and investigate its coupling and co-variations with the OWP. The joint examination of the area variations, centroid locations, and zonal migrations of the AWP and OWP lead to a number of interesting findings. The results hopefully can contribute to our understanding of the air-sea interaction in general and characterization of El Niño/La Niña events in particular.

Keyword: OWP (The oceanic warm pool); AWP (atmospheric wet pool); air-sea interaction

1 INTRODUCTION

The interaction between the ocean and atmosphere plays important roles in climate variation. The most intensive air-sea interaction region is located in the Indio-Pacific oceanic warm pool (OWP) area with sea surface temperature (SST) above 28°C. The OWP region has become one of the focused regions for scientific studies on climate variability, in particular after scientists realized that it has a close relationship to El Niño—Southern Oscillation (ENSO) (Wyrtki, 1982; Philander, 1990; Picaut et al, 1996; Yan et al, 1997; McPhaden, 1999).

Yan et al. (1992a, b; 1993) first studied the variability of the western Pacific warm pool (WPWP) by examining its size, temperature, and eastern boundary with satellite SST data, and they concluded that remote sensing data are very effective and efficient in investigating the variation of WPWP. Ho et al. (1995) used the joint measurements of SST from Advanced Very High Resolution Radiometer (AVHRR) infrared data and sea level from Geosat to investigate the upper-layer variability of the WPWP. Yan et al. (1997) further tracked the centroid trajectory of the WPWP during three El Niño events by using AVHRR pathfinder satellite data. All these studies have largely improved our knowledge of the warmest portion in the ocean.

However, studies on the mirror of the OWP termed atmospheric wet pool (AWP) where the largest accumulation of water vapor (WV) in the atmosphere is observed are limited. Using joint analysis of SST and WV to study the co-variation of the OWP and AWP in the air-sea system is rare, although previous investigations suggest that analyses on other geophysical parameters with SST in the "pool" context might be an effective and efficient approach to understanding the air-sea interaction (Chen et al., 2004). In this study, we jointly analyzed the simultaneous observations of SST and WV to examine the characteristics of the AWP and the co-variation of the OWP and AWP, in order to achieve a better understanding of the interaction of the ocean and atmosphere in general and delineation of El Niño / La Niña events in particular. In the following sections, unless we mention otherwise, the abbreviations, the OWP and AWP refer to the Indio-Pacific "pools", whereas the WHOWP and WHAWP denote the western hemisphere (WH) "pools", respectively.

* Supported by the National Natural Science Foundation of China under projects (Nos. 40730530, 40675016, 40706056)
** Corresponding author: zhangcy@utdallas.edu

2 DATA

We compiled 14-year simultaneous observations of SST and WV from January 1988 to December 2001 covering 30°S–30°N, 40°E–300°E on the basis of 168-month collated fields at 1°×1° grid. Two datasets are described as follows.

1) Reynolds et al. (2002) SST dataset. Monthly SST data of the ocean at 1°×1° grid are derived from Physical Oceanography Distributed Active Archive Center (PO DAAC), and National Aeronautics and Space Administration (NASA). The NCEP Reynolds Optimally Interpolated SST Version 2 (OISST V2) products consist of weekly and monthly global SST fields, which blends both *in situ* and AVHRR satellite derived SSTs. The satellite derived SSTs are from the Multichannel SST products that have been constructed operationally from the five-channel AVHRR by NOAA's Environmental Satellite. A 14-year dataset from January 1988 to December 2001 have been compiled in this study to collate with the simultaneous measurements of WV.

2) NVAP columnar WV dataset. NASA Water Vapor Project (NAVP) (Randel et al., 1996) datasets comprise a combination of radiosonde observations, Television and Infrared Operational Satellite (TIROS) Operational Vertical Sounders (TOVS), and Special Sensor Microwave/Imager (SSM/I) datasets. Up to date, they are the best observations available for WV. We first subtracted 12-year (1988–1999) monthly 1°×1° gridded columnar WV data and 2-year (2000–2001) monthly 0.5°×0.5° next generation gridded WV data from the NVAP WV products. To obtain 14-year (1988–2001) monthly 1°×1° gridded WV data, the next generation data were resampled to 1°×1° grid. Finally, the NVAP monthly gridded WV dataset over the ocean was compiled so that it can be collated with the SST observations during the same period.

3 THE ATMOSPHERIC WET POOL

The OWP, defined as a closed region with SST above 28°C, is known as the "heat reservoir" in the ocean or the "firebox" in the atmosphere. The warmest portion in the ocean mirrors the fact that the wettest region with the largest accumulation of WV in the atmosphere, termed atmospheric wet pool (AWP), should be identified because the ability of atmosphere to hold water vapor increases nonlinearly with temperature, which is known as the Clausius-Clapeyron relationship between SST and WV. The geographical distributions of SST and WV support this relationship between these two variables, as illustrated (Fig.1).

Two parameters share many similarities in geographical distributions. First, both of them basically follow a zonal pattern, decreasing from the equator to off-equatorial region. Second, the zonal gradient is prominent in both of them, especially in the Pacific and third, the well-known OWP is found to be well mirrored in the atmosphere by the AWP, where the wettest atmosphere is observed due to the largest accumulation of WV over that region, suggesting the strong coupling of the ocean and atmosphere in this region. The OWP and AWP both have a double-tongue structure at their east boundaries, and the AWP looks smaller than the OWP in area if we limit it to a closed region. Aside from these two large pools, the second warm pool in the ocean located in the WH, abbreviated as the WHOWP, also has a small WH atmospheric wet pool (WHAWP) as a mirror in the atmosphere. Obvious shift between these two small pools in their geographic locations is observed with the WHAWP lying in the far south of the WHOWP, suggesting a different dynamical process in developing these two AWPs in the atmosphere.

The threshold of the OWP is selected as 29°C (McPhaden and Picaut, 1990) or 28°C (Ho et al., 1995) based on limiting it to a closed region with an extensively high SST, and the thresholds such as 27.8°C and 28.2°C have no significant change in the shape and the relative positions of the WPWP (Yan et al., 1997). With the similar considerations of the OWP in selecting the threshold, it seems that the threshold for the AWP should be around 50 mm, at least in a climatological sense. The selections such as 49.5 mm and 50.5 mm have no significant change for.

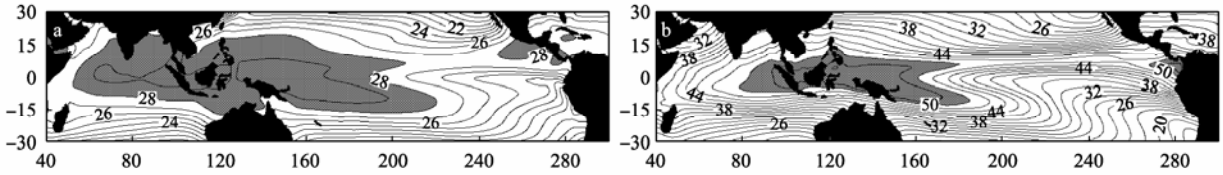

Fig.1 Climatologies (1988–2001) for (a) SST (°C)**; (b) water vapor** (mm) **derived from OI SST V2 and NVAP, respectively**

The OWP and AWP are shaded. The contour interval for SST is 1°C and for water vapor is 2 mm

tracking the centroid movements and the relative positions of the AWP either (Zhang, 2007). Therefore we define the AWP as a closed atmospheric area with total column WV above 50 mm.

Recently, Chen et al. (2008) proposed to use 28.5°C as the threshold of the WPWP given the large ocean climate shift happened around 1979. They also argued that the new threshold is more reasonable since it can better characterize the features of this climate shift. In this study, we used the traditional 28°C as the threshold to define OWP and WHOWP since the selection of 28°C and 28.5°C has no large impact on the areas and centroid locations of OWP and WHOWP if we define the OWP within the range of 40°E–250°E, 30°S–30°N and WHOWP within the range of 250°E–300°E, 0°S–30°N.

In the next section, detailed comparisons of OWP/AWP and WHOWP/WHAWP in their seasonal evolutions, centroid movements, area variations, and co-variations in El Niño/La Niña events are presented.

4 COMPARISON OF THE OWP AND AWP

4.1 Seasonal evolution

The climatologically seasonal distributions of SST and WV during 1988–2001 are plotted in Fig.2. We can see that both the OWP and AWP undergo a distinct seasonal evolution in their geographical extensions and relative positions. Two pools share a systemic consistence in meridional seesaw with their northernmost and southernmost migrations occurred in June-August (JJA) and December-February (DJF), respectively, which suggests the couplings of these two pools. However, the intra-annual variations of them are different both in their shapes and intensities. The OWP maximizes/minimizes its thermal core with SSTs above 29°C in March-May (MAM)/DJF by extending/shrinking its area mainly in zonal orientation, whereas large intra-annual variation of the AWP is mainly occurred in the meridional orientation. This is caused by the strong regional enhancement/decline of vapor density between JJA and DJF over the Asian monsoon area, which can induce large rainfall/drought over that area.

The WHOWP starts to develop in MAM and reaches its maximum in JJA by expending to the Gulf of Mexico and Caribbean and western tropical North Atlantic. In September-November (SON), it begins to decay by disappearing from the Gulf of Mexico and disappears completely in DJF. As far as the WHAWP is concerned, the seasonal evolution is consistent with the WHOWP, however, three prominent features can be observed. First, the WHAWP is always located to the south of the WHOWP for a whole year. Second, the WHAWP can hardly cross the intra-Americas landmass even though it seems easier to occur than that of the WHOWP since it is located in the atmosphere and

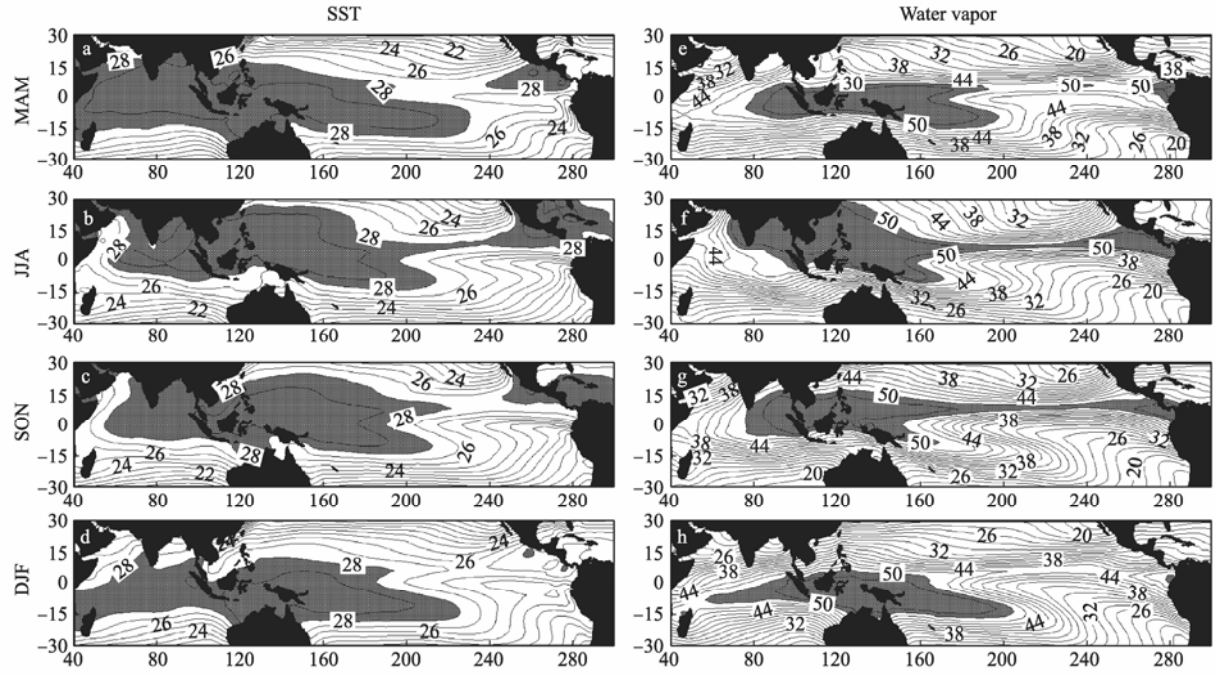

Fig.2 14-yr (1988–2001) **quarterly averaged SST** (°C)**, and water vapor** (mm)**. Data are from OI SST V2 and NVAP, respectively**
The OWP and AWP are shaded. The contour interval for SST is 1°C and for water vapor is 2 mm

third, the meridional seesaw is more significant than the WHOWP. The roles of the WHOWP in the climate have been received considerable concerns (Wang and Enfield, 2001; 2003). According to Wang and Enfield (2003), the seasonal development of the WHOWP is induced primarily by the annual variations of the surface net heat flux over that region; meanwhile, the warm water also has a significant impact on organized tropical convection that is associated with atmospheric convergence/divergence and vertical motion. It therefore can be concluded that these observed differences between the WHOWP and WHAWP are closely connected with the adjacent Harley and Walk circulation cells as suggested previously by Wang and Enfield (2003).

4.2 Centroid motion

The thermal centroid of the WPWP is indicated to be closely linked to the onset of the El Niño event and the air-sea interaction because its location is controlled by the overall shape and position of the WPWP (Ho et al., 1995; Yan et al., 1997). Following the implications of previous studies related to the centroid motion of the WPWP, the centroids of OWP/AWP and WHOWP/WHAWP during 1988–2001 are computed in terms of a new scheme proposed by Chen and Fang (2005) as follows.

$$x = \frac{\sum_{i=1}^{n} w_i x_i}{\sum_{i=1}^{n} w_i} \tag{1}$$

$$y = \frac{\sum_{i=1}^{n} w_i y_i}{\sum_{i=1}^{n} w_i} \tag{2}$$

$$w_i = \frac{T_i - T_{\min}}{T_{\max} - T_{\min}} \tag{3}$$

where x and y denote the zonal and meridional components of the centroid location of each pool, respectively. x_i and y_i are the zonal and meridional positions of each pixel with SST≥28°C or WV ≥50 mm, and n is the total number of pixels of each pool. w_i is a normalized weighting for pixel i. T_i is the SST/WV value of pixel i, $T_{\max}$ and $T_{\min}$ are the maximum and minimum SST/WV values within each pool, respectively.

The significant improvement for tracking the centroid location of each pool by using this new scheme is the interference of w_i by considering the inner structure of each pool, which was neglected in the scheme employed by Ho et al. (1995) and Yan et al. (1997) because they just considered the shape of the outer boundary of the WPWP and assumed that the inner structure of the WPWP was consistent. The zonal and meridional components of the thermal and wet centroids of the OWP/AWP, WHOWP/WHAWP are plotted in Fig.3 and Fig.4, respectively.

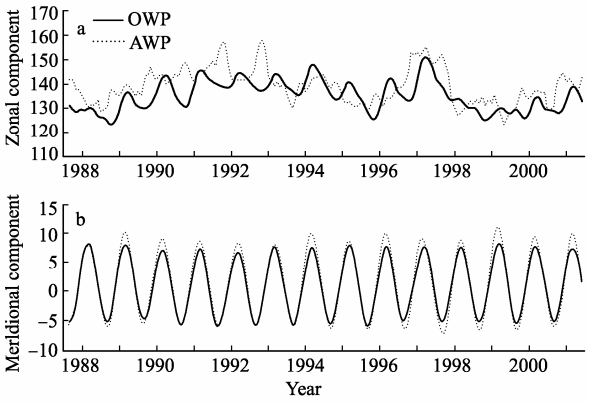

Fig.3 Monthly time series of zonal (top panel) **and meridional components** (bottom panel) **of the centroid locations of the OWP and AWP from January 1988 to December 2001**

The computing range is based on 40°E–250°E, 30°S–30°N. The thresholds for the OWP and AWP are selected as 28°C and 50mm, respectively

It can be seen that the thermal centroid undergoes a prominent annual cycle and secondary interannual variation generally after three-month running mean is applied (Fig.3a). Unlike the centroid motion of the WPWP (Yan, et al, 1997), which is more sensitive to El Niño events by largely shifting eastward during the warm events, the migration of the thermal center of the OWP is inertial for these large interannual variations. Only small eastward shifts have been observed during the El Niño years. However during the 1997/1998 El Niño event, the largest warm event in records, the thermal centroid indeed underwent the largest eastward migration in the zonal component during 1988–2001. This difference between the WPWP and OWP in their centroid motions suggests the important roles of the Indian warm pool in maintaining the relative centroid position as well as the shape of the OWP. A comparison of the centroid motion between the WPWP and OWP illustrates an out-of-phase relationship between them (Zhang, 2007). The centroid motion of the AWP is consistent with that of the OWP at annual and interannual time scales; however, three distinguished differences can be found. First, the wet centroid is located to the east of the thermal centroid in a majority of months during 1988–2001. Second, the intra-annual

variations of the wet centroid are more significant and the semiannual variation is obviously observed. Third, a general out-of-phase relationship is observed between the wet and thermal centroid for some years, such as 1991, 1992 and 1993. Finally, the wet centroid underwent a significant eastward migration during the 1991/1992, 1992/1993, and 1997/1998 El Niño events. As far as the meridional component is concerned (Fig.3b), only annual cycle is dominant. This is caused by the strong annual solar cycle. We also note that the wet centroid can reach higher latitudes than the thermal centroid does, which is mainly induced by the enhancement of the vapor density over the Asian monsoon region.

The centroid motion of the WHOWP and WHAWP has never been documented in the literature. The zonal component of the centroid motion of the WHOWP/WHAWP is primarily dominated by annual cycle and secondarily by semiannual cycle/quasi-semiannual cycle. The zonal fluctuation of two pools is consistent in their zonal range (Fig.4a). However, their phase is inconsistent with an out-of-phase relationship being observed in a majority of months. In the meridional component, their oscillations are consistent with the wet centroid located to the south of the thermal centroid. The annual cycle also dominates the meridional variation and the semiannual variation also can be observed, in particular for the WHAWP (Fig.4b).

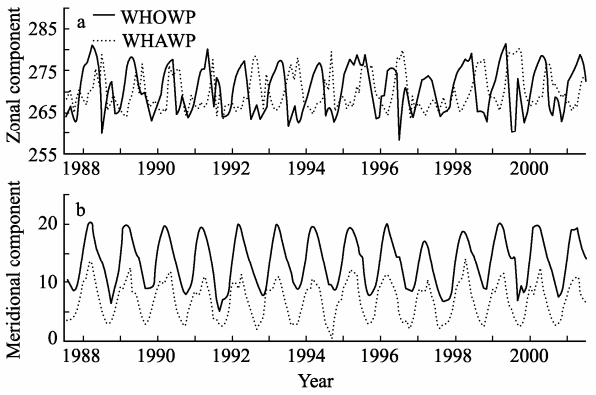

Fig.4 Monthly time series of zonal (top panel) **and meridional components** (bottom panel) **of the centroid locations of the WHOWP and WHAWP from January 1988 to December 2001**

The computing range is based on 250°E–300°E, 0°S–30°N The thresholds for the WHOWP and WHAWP are selected as 28°C and 50 mm, respectively

4.3 Area evolution

The grid points with SST/WV above 28°C/50 mm for the OWP/AWP and WHOWP/WHAWP are derived and presented in Fig.5. As can be seen in Fig.5a, the variations of the OWP and AWP in area are much consistent in their first dominant annual variation with the AWP systematically lower than the OWP, which have been implied in Fig.1 that the area of OWP is larger than the AWP based on the threshold of 50 mm for water vapor. The semiannual variation in the OWP is distinct, which reaches its first peak in April and second peak in September with the first stronger than the second, suggesting the direct impact of the semiannual component of solar irradiance on tropical region by noting that the Sun crosses the equator twice during a year. However, this semiannual component is not well mirrored in the AWP since the intra-annual variation is active in a higher-frequency mode for the AWP. This may be caused by the sensitivity of vapor in the atmosphere or the SST data is smoother than the WV data used in this study. The El Niño and La Niño events have impact on their area evolutions by noting that both pools become larger/smaller during El Niño/ La Niña years.

As far as the WHOWP and WHAWP in area variation are concerned, two pools are much consistent with the annual cycle as the primary mode, which is slightly modulated by the semiannual cycle (Fig.5b). Their phases in reaching their maximums and minimums undergo a large interannual variation. The annual consistence in their area evolutions mainly attributes to their persistent locations in the NH that hardly cross the equator. It is interesting to find that both pools reach their largest area in the 1997/1998 El Niño event, suggesting that El Niño can enhance the magnitude of the WH pools. We, however, have not observed obvious impacts of La Niña on these two pools yet.

4.4 Variations during El Niño and La Niña

El Niño / La Niña events can influence the variation of the centroids and areas of the OWP and AWP. Previous studies concluded that the interannual variations of the WPWP (McPhaden and Picaut, 1990; Ho et al., 1995) and AWP (Chen, 2004) are characterized by a zonal oscillation of their central positions. It can therefore be anticipated that geographical correlations of these “pools” may be better illustrated by their behaviors during El Niño and La Niña years. During 1988–2001, the years 1991, 1992, 1994 and 1997 are dominated by El Niños, whereas La Niñas prevail 1988, 1999 and 2002. The annual average SST and WV for the composite El Niño years and La Niña years are shown in Fig.6.

The geographical distributions of SST and WV, like other geophysical parameters, illustrate three climate modes on interannual time scale, El Niño mode (Fig.6a and b), normal mode (Fig.1) and La Niña mode (Fig.6c and d). The OWP and AWP exhibit a systemic eastward migration during El Niño years and a westward contraction during La Niña years. The displacement can reach approximate 20° in longitude between El Niño and La Niña years. The AWP varies more significantly than the OWP in shape during El Niño years. Another striking feature is the pronounced variations of the WHOWP and WHAWP with enhanced/declining magnitude both in intensity and area during El Niño / La Niña years.

The large zonal oscillations of the OWP and AWP on interannual time scale are mainly attributed to the ENSO phenomenon (Lau, 1997). The migration of the OWP and its overlying convection are fundamental to ENSO (McPhaden and Picaut, 1990). This migration was generally associated with the wind-driven zonal current advection in the tropical ocean. To help understand this mechanism, the SST and WV anomalies for the composite El Niño and La Niña years relative to their respective 14-yr climatologies are shown in Fig.7. Several notable features are easily identifiable in Fig.7. First, dipole-like patterns in the SST and WV are observed with a sign-opposite structure for these two climate modes. Second, the maximum and minimum anomalies of two parameters are located in the central equatorial Pacific, instead of the eastern equatorial Pacific, where large SST anomaly accompanying with slight vapor has been observed. Third, a close inspection reveals that the maximum/minimum vapor anomaly during warm/cold events is located west of the maximum/minimum SST anomaly. Finally the El Niño pattern is anticorrelated with the La Niña pattern. Bearing these features in mind, we can continue to discuss the zonal oscillation of two pools in anomalous context. According to McPhaden and

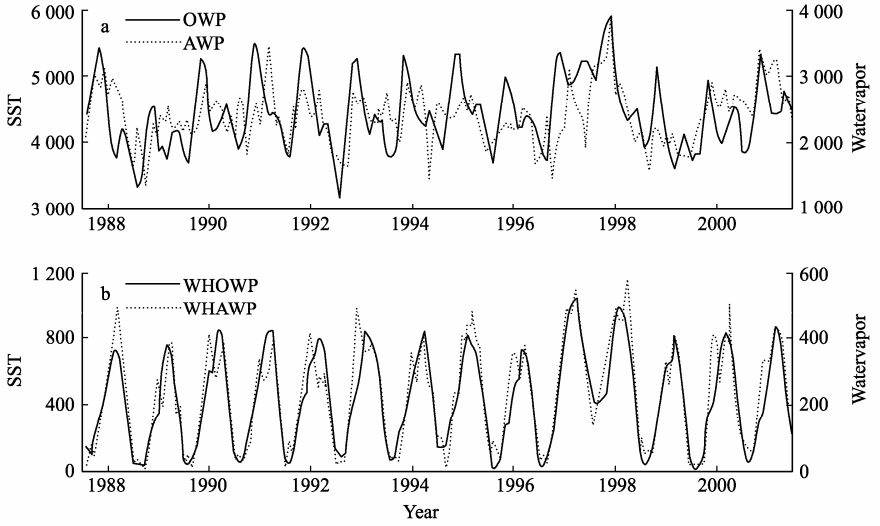

Fig.5 Area evolutions for (a) **the OWP and AWP,** (b) **the WHOWP and WHAWP**

The computing range of the OWP and AWP is based on 40°E–250°E, 30°S–30°N, and the WHOWP and WHAP is based on 250°E–300°E, 0°–30°N. The thresholds for the OWP/WHOWP and AWP/WHAWP are selected as 28°C and 50 mm, respectively

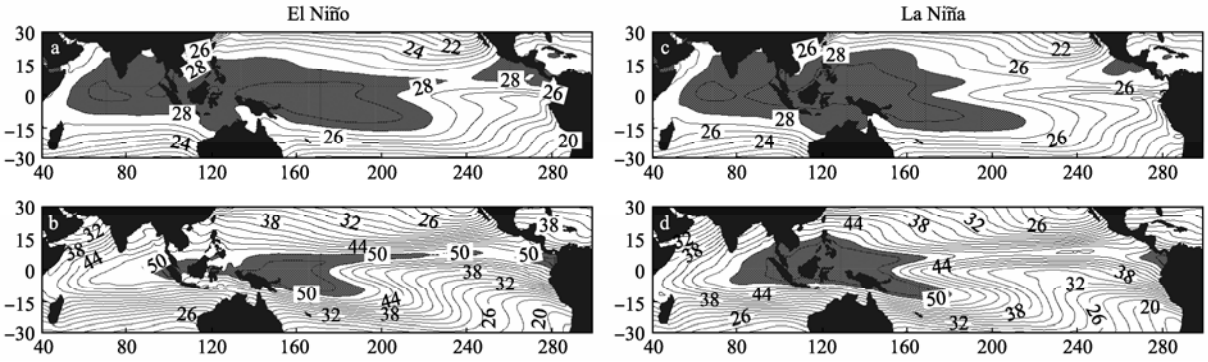

Fig.6 Averaged SST (°C) **for the composite** (a) **El Niño** (1991, 1992, 1994 and 1997)**, and** (c) **La Niña** (1988, 1999 and 2000) **years during 1988-2001.** (b) **and** (d) **are similar maps but for water vapor** (mm)

The OWP and AWP are shaded. The contour interval for SST is 1°C and for water vapor is 2 mm

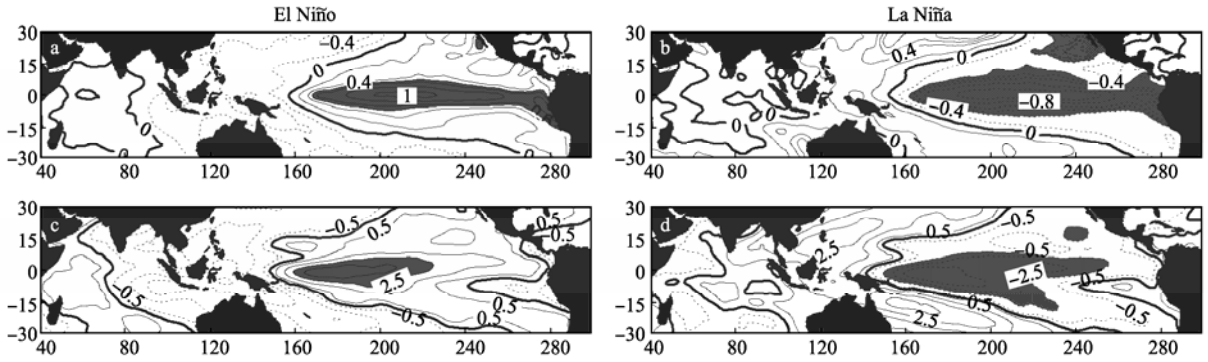

Fig.7 SST (°C) **anomalies with respect to 14-yr climatology** (1988-2001) **for the composite** (a) **El Niño** (1991, 1992, 1994 and 1997)**, and** (c) **La Niña** (1988, 1999 and 2000) **years;** (b) **and** (d) **are similar maps but for water vapor** (mm)
The positive and negative high anomalies are shaded. The thin solid, dotted and thick curves denote the positive, negative and zero contours, respectively. The contour interval for SST anomaly is 0.2°C and for water vapor anomaly is 1.0 mm

Picaut (1990), warm SST anomaly in the equatorial Pacific can generate anomalous deep atmospheric convection by convergence of trade winds over the surface. Then the convergence leads to a weakening of trade winds west of warm SST anomaly. The ocean responds rapidly to this weakening: surface currents locally accelerate eastward, and large-scale equatorial Kelvin and Rossby waves radiate out from the directly forced region to reinforce and spread the warm SST anomaly across the basin. The positive feedback between the ocean and atmosphere continues until easterly trade winds return to their full strength. The entire process may last 12–18 months during which a cycle of zonal oscillation of the OWP and AWP can be finished.

For examining the synchronized zonal migration of the OWP and AWP, the time/longitude diagrams of the SST and WV are plotted for 1988–2001, as shown in Fig.8. It can be seen that the dateline can roughly serve as a dividing line between two characteristic regimes. East to the dateline, cold features of SST, dry features of WV appear to propagate westward consistently with a regular seasonal fluctuation in intensity. This seasonal migration of the SST and WV though propagate coherently in time, they are in different mechanism. The cold and dry cores are well separated during the propagation with the cold core locating around 270°E and dry core defined by the WV anchoring at 230°E. Note that small wet region induced by the WHAWP in the eastern equatorial Pacific also undergoes a seasonal westward migration regularly (Fig.8b). The cold SST propagation is closely associated with the South Equatorial Current which carries the cold upwelling water from the Peruvian coast, which can induce a series of tongue-shaped contours in the eastern equatorial Pacific (Fig.1a). The cold SST in the ocean and low precipitation in the atmosphere together form a poor convection and low atmospheric vapor content over that region. This is caused because the relationship of the SST and saturation vapor pressure is nonlinear. There is a dramatic increase in atmospheric vapor content and atmospheric convection when SST above 28°C. The low precipitation-related latent heat further decreases the atmospheric capability in lading vapor content. This low vapor content region also has a normally annual westward migration. West to the dateline, however, the evolution of SST and WV is dominated by large scale interannual variations. The thermal and wet cores of the OWP and AWP are found to wander zonally from year to year with a weak annual cycle in their intensities. However, small discrepancy still can be observed during their eastward migrations. The OWP crosses the Pacific basin with a declining intensity, while the AWP propagates in increasing strength and reaches its maximum in the eastern and central Pacific. Note that during the onset of the 1997/1998 El Niño event, decreased SST and WV have been observed simultaneously over the western Pacific, which is more obvious in WV. This decrease is closely associated with the bursts of westerlies in the western Pacific, which can excite the equatorial Kelvin waves and therefore potentially lead to the onset of an El Niño event. These anomalous westerlies have more impacts on the atmospheric parameter WV than the oceanic variable SST because the ocean needs longer time to adjust its status to the atmospheric forcing. For a better understanding of this process, the corresponding time/longitude diagrams of the zonal and meridional components of the sea surface wind speed derived from ERS-1/ERS-2 (CERSAT, 2002) are plotted (Fig.9).

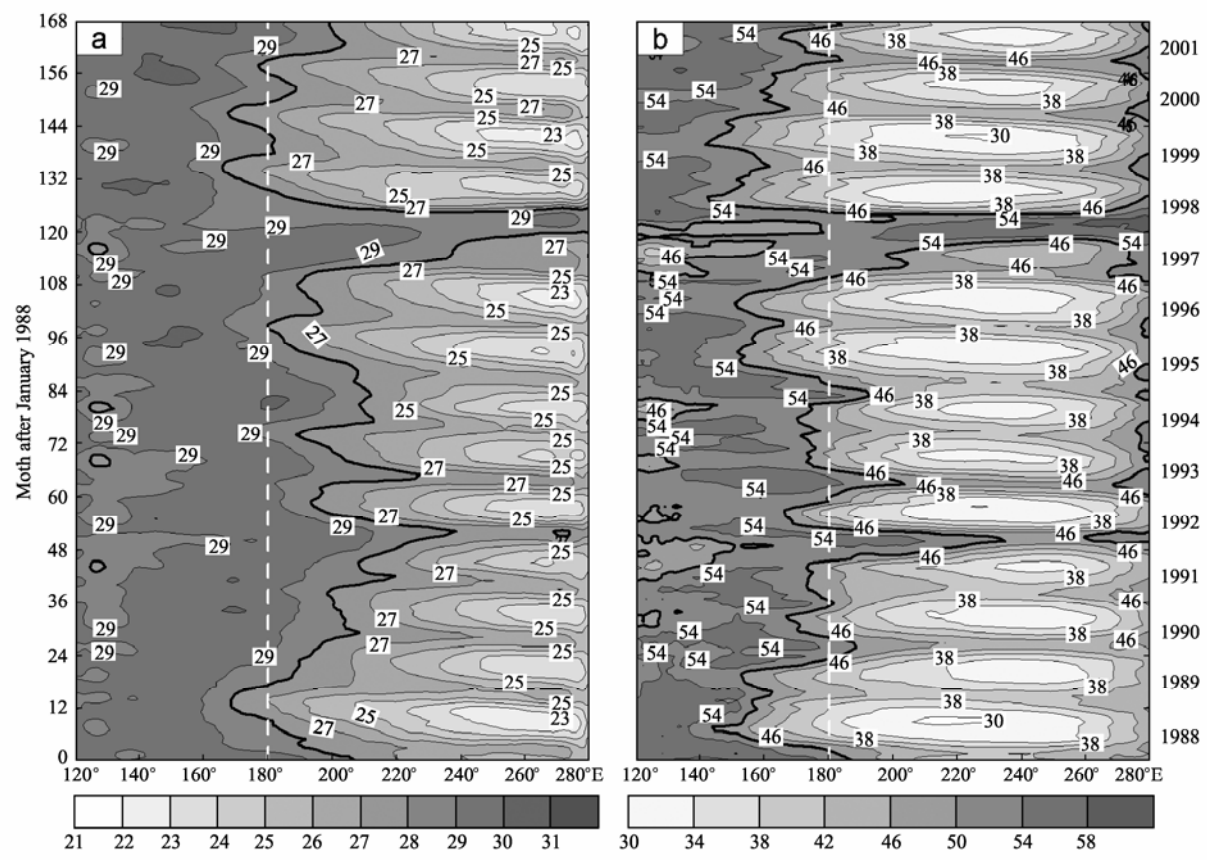

Fig.8 Time/longitude diagrams for (a) **SST** (°C)**, and** (b) **water vapor** (mm) **along the equatorial Pacific** (averaged between 5°S and 5°N)

The thick solid curves in (a) and (b) denote the contours of 28°C and 50 mm for SST, and water vapor, respectively. The vertical dashed lines in (a) and (b) indicate the dateline. The contour interval for SST is 1°C and for water vapor is 4 mm

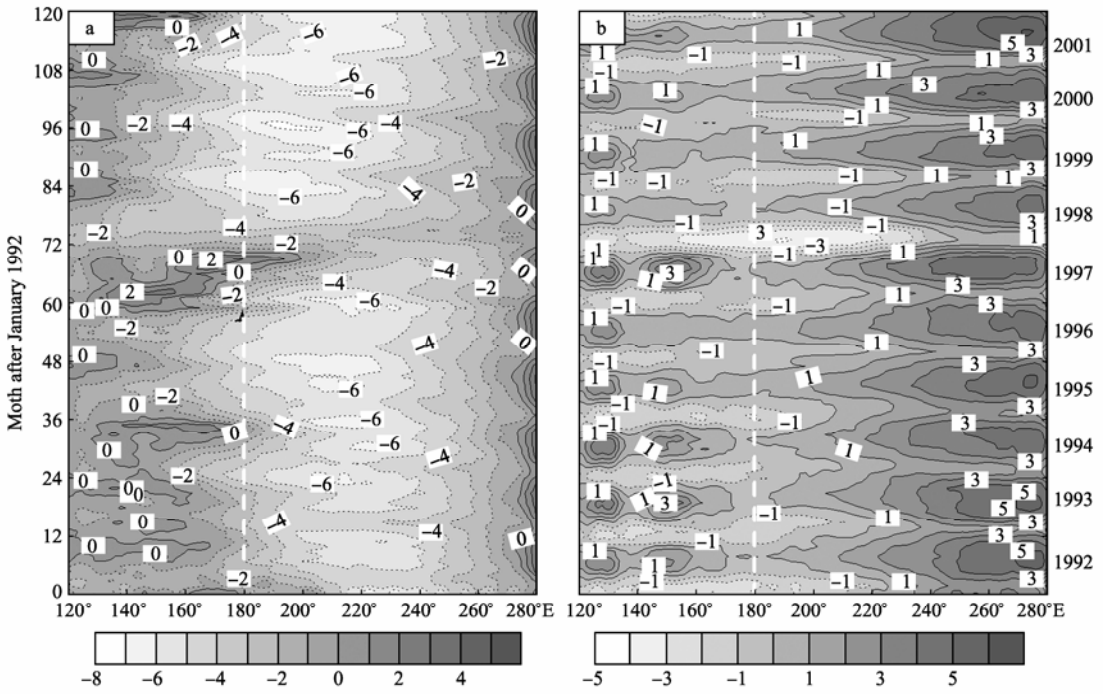

Fig.9 Time/longitude diagrams for (a) **zonal and** (b) **meridional sea surface wind speed** (m/s) **along the equatorial Pacific** (averaged between 5°S and 5°N)

Positive (negative) winds are westerly (easterly) and southerly (northerly) in (a) and (b), respectively. The vertical dashed lines in (a) and (b) indicate the dateline. The contour interval is 1 m/s

The zonal wind along the equatorial Pacific is dominated by westerlies over the western and eastern Pacific, while by easterlies over the central Pacific. This zonal wind undergoes an annual cycle and significant interannual variation, especially during El Niño events. In 1997, this basic zonal wind pattern has been significantly violated by the intensified westerlies over the western Pacific pool region, meanwhile, this bursting westerly propagated eastward until 200°E (Fig.9a). This strong westerly will lead to a strong zonal advection and a large eastward displacement of deep convection; therefore, a strong eastward of rain zone would be formed. The weakening of the SST and vapor content in the western Pacific is closely associated with this westerly wind burst. Eastward ocean current is also forced by the strong westerlies; therefore, a striking zonal migration of the OWP occurs as an adjustment of the ocean to the atmospheric forcing. As far as the meridional component of the wind field is concerned, the equatorial Pacific is strongly controlled by the southerly to the east of the dateline, and exception occurs during the first of several months in 1998 when the northerly prevails almost in the entire equatorial Pacific. Note that this exception occurs just after the termination of the enhanced westerly. Therefore it can be argued that the anomalous intensification and migration of the westerly in the western Pacific accompany with the onset of the 1997/1998 El Niño event, while the demise of this event is associated with a sudden reversal of meridional wind from southerly to northerly along the equatorial Pacific.

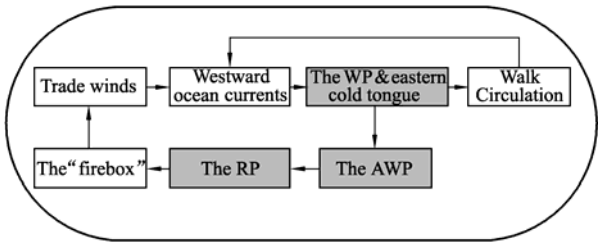

Fig.10 Schematic map of the coupled air-sea system revealed by the OWP and AWP over the tropical Indian-Pacific basin

5 SUMMARY AND DISCUSSIONS

In this paper, the wettest atmospheric zone, termed atmospheric wet pool (AWP) is defined and its comparison with the OWP is studied. The AWP is defined as a closed region with the total column of WV more than 50 mm. By jointly analyzing the simultaneous observations of WV and SST during 1988–2001 in a pool context, a series of interesting findings are presented.

First, the AWP well mirrors the OWP and the coupling of these two pools can effectively and efficiently reveal the interaction of the ocean and atmosphere in the tropical region. As we know, the OWP is formed due to the tropical ocean currents forced by the trade winds together with a series of ocean dynamic processes happened in the western Pacific. The subsequent SST pattern in the tropical ocean helps with the development of the Walk Circulation in the atmosphere. A coupled positive feedback between the ocean and atmosphere maintains the state of the tropical Pacific. In this positive system, the OWP behaves like a heat pump to exert energy and heat into the atmosphere, which largely increases the temperature and therefore the capability of lading WV of the atmosphere. Therefore, the largest accumulation of WV area is developed over the OWP region. The warm atmosphere loading with heavy WV tends to rise, expand and cool, and it is no longer able to hold as much moisture as it reaches some height. The moisture then begins to condense into water droplets and raining cloud system will grow rapidly over this warmer SST region. Thus, the maximum annual precipitation is developed over the OWP, which is termed the rain pool (RP). This heavy rainfall over the OWP region can further induce a large release of latent heat into the atmosphere, which can be used by the ocean in turn through the wind system because the wind system gets most of its energy from this released latent heat. The observed OWP, AWP and RP under normal conditions without ENSO events attribute to a series of positive feedbacks in the tropical air-sea system, which can be schematized in Fig.10. In turn, the existence of these pools well illustrates the intensive interaction of the ocean and atmosphere over this region.

Second, although the AWP and OWP undergo many similarities in their spatial structures, annual variation in areas, intensities and centroid movements, the coherent trans-Pacific propagations during 1997/1998 El Niño event, as well as the dipole mode in composite El Niño / La Niño years due to the coupling effects between them, many differences still can be identified. First, the AWP is always smaller than the OWP in area. Second, the seasonal variation of the AWP is significantly occurred in the meridional orientation instead of in the zonal orientation, which is opposite to the OWP annual variation. Third, the AWP is easier to change its

geographical locations, area variations and centroid movements on intra-annual time scale. Fourth, the centroid motion of the OWP/AWP and WHOWP/WHAWP undergoes a general out-of-phase relationship in the zonal component, and the wet center of the AWP propagates more eastward than the thermal center of the WP during the 1997/1998 El Niño event. Finally, although positive/negative anomalies have been observed in the central equatorial Pacific during the composite El Niño/La Niña years, large displacements have been observed among the anomaly cores in their zonal locations, with the vapor anomaly core being around 178°E, and the SST anomaly core anchoring the easternmost position around 208°E in El Niño and 192°E in La Niña years, respectively.

Aside from two pools in the EH have been well mirrored each other in the coupled air-sea system, another pair of pools in the WH also have been strikingly revealed. Unlike their associated EH ones, they all locate in the NH, with the WHAWP straddling approximately 5° south of the WHOWP. Their area evolutions and centroid motions are firstly investigated and show pronounced annual cycles in variability. According to Wang and Enfield (2001), the seasonal evolution of the WHOWP is induced primarily by the surface net heat flux over that region, but the secondary roles of reduced entrainment cooling, in general, and advection in the eastern North Pacific, deserve their further attention. They also suggested that as the WHOWP develops and rainy season begins, warmer SSTs are associated with a warmer and moister troposphere, reduced sea level pressure, weaker easterly trade winds, which can cause the development of the WHAWP in the atmosphere by air-sea interaction. However, the geographical shift in their locations deserves our further studies.

References

CERSAT. CERSAT user manual: Mean wind fields (MWF Product), volume 1. ERS-1, ERS-2 and NSCAT. Plouzane´, France: C2-MUTW-05-IF, Version 1.0, 2002.

Chen, G., 2004. A 10-yr climatology of oceanic water vapor derived from the TOPEX microwave radiometer. *Journal of Climate* **17**: 2 541-2 557.

Chen, G., C. Fang, C. Zhang and Y. Chen, 2004. Observing the coupling effect between warm pool and "rain pool" in the Pacific Ocean. *Remote Sensing of Environment* **91**: 153-159.

Chen, G. and L. Fang, 2005. Improved scheme for determining the thermal centroid of the oceanic warm pool using sea surface temperature data. *Journal of Oceanography* **61**: 295-299.

Chen, J., N. Wang and X. Lv, 2008. Spatial and temporal distribution of the western Pacific warm pool and its relationship with ENSO cycle. *Acta Oceanologica Sinica* **30**: 10-19.

Ho, C. R., X. H. Yan and Q. Zheng, 1995. Satellite observations of upper-layer variability in the western Pacific warm pool. *Bulletin of the American Meteorological Society* **76**: 669-679.

Lau, N. C., 1997. Interactions between global SST anomalies and the midlatitude atmospheric circulation. *Bulletin of the American Meteorological Society* **78**: 21-33.

McPhaden, M. J., 1999. Genesis and evolution of 1997-1998 El Niño. *Science* **283**: 950-953.

McPhaden, M. J. and J. Picaut, 1990. El Niño-Southern Oscillation displacements of the western equatorial Pacific warm pool. *Science* **250**:1 385-1 388.

Philander, S. G. H., 1990. El Niño, La Niña, Southern Oscillation. USA: Academic Press, 293.

Picaut, J., M. Ioualalen, C. Menkes, T. Delcroix and M. J. McPhaden, 1996. Mechanism of the zonal displacement of the Pacific warm pool: Implication for ENSO. *Science* **274**:1 486-1 489.

Randel, D. L., T. H. Vonder Haar, M. A. Ringerud, G. L. Stephens, T. J. Greenwald and C. L. Combs, 1996. A new global water vapor dataset. *Bulletin of the American Meteorological Society* **77**: 1 233-1 246.

Reynolds, R. W., N. A. Rayner, T. M. Smith, D. C. Stokes and W. Wang, 2002. An improved in situ and satellite SST analysis for climate. *Journal of Climate* **15**: 1 609-1 625.

Wang, C. and D. B. Enfield, 2001. The tropical Western Hemisphere warm pool. *Geophysical Research Letters,* 28: 1 635-1 638.

Wang, C., and D. B. Enfield, 2003. A further study of the tropical Western Hemisphere warm pool. *Journal of Climate* **16**: 1 476-1 493.

Wyrtki, K., 1982. The Southern Oscillation, ocean-atmosphere interaction and El Niño. *Marine Technology Society Journal* **6**: 3-10.

Yan, X. H., V. Klemas and D. Chen, 1992a. The western Pacific warm pool observation from space. *EOS Transaction* **74**: 41-44.

Yan, X. H., C. R. Ho, Q. Zheng and V. Klemas, 1992b. Temperature and size variabilities of the western Pacific warm Pool. *Science* **258**: 1 643-1 645.

Yan, X. H., C. R. Ho, Q. Zheng and V. Klemas, 1993. Using satellite infrared data in studies of variabilities of the western Pacific warm pool. *Science* **262**: 440-441.

Yan, X. H., Y. He, W. T. Liu, Q. Zheng and C. R. Ho, 1997. Centroid motion of the western Pacific warm pool during three recent El Niño-Southern Oscillation events. *Journal of Physical Oceanography* **27**: 837-845.

Zhang, C., 2007. Study of low-frequency variations and interactions in the air-sea system. Ph.D. dissertation, Ocean University of China, Qingdao, China, pp. 62-91.